Inorg. Chem. **2006**, *45*, 5338–5350

Synthesis, Structure, and Magnetic Properties of (6–9)-Nuclear Ni(II) Trimethylacetates and Their Heterospin Complexes with Nitroxides

Victor Ovcharenko,*,† Elena Fursova,†,‡ Galina Romanenko,† Igor Eremenko,§ Evgeny Tretyakov,† and Vladimir Ikorskii†

International Tomography Center, Russian Academy of Sciences, 3A Institutskaya Street, 630090 Novosibirsk, Russia, Novosibirsk State University, 2 Pirogova Street, 630090 Novosibirsk, Russia, and N. S. Kurnakov Institute of General and Inorganic Chemistry, Russian Academy of Sciences, Moscow, Russia

Received December 28, 2005

New polynuclear nickel trimethylacetates $[Ni_6(OH)_4(C_5H_9O_2)_8(C_5H_{10}O_2)_4]$ (**6**), $[Ni_7(OH)_7(C_5H_9O_2)_7(C_5H_{10}O_2)_6(H_2O)]\cdot 0.5C_6H_{14}\cdot 0.5H_2O$ (**7**), $[Ni_8(OH)_4(H_2O)_2(C_5H_9O_2)_{12}]$ (**8**), and $[Ni_9(OH)_6(C_5H_9O_2)_{12}(C_5H_{10}O_2)_4]\cdot C_5H_{10}O_2\cdot 3H_2O$ (**9**), where $C_5H_9O_2$ is trimethylacetate and $C_5H_{10}O_2$ is trimethylacetic acid, have been found. Their structures were determined by X-ray crystallography. Because of their high solubility in low-polarity organic solvents, compounds **6**–**9** reacted with stable organic radicals to form the first heterospin compounds based on polynuclear Ni(II) trimethylacetate and nitronyl nitroxides containing pyrazole (L^1–L^3), methyl (L^4), or imidazole (L^5) substituent groups, respectively, in side chain $[Ni_7(OH)_5(C_5H_9O_2)_9(C_5H_{10}O_2)_2(L^1)_2(H_2O)]\cdot 0.5C_6H_{14}\cdot H_2O$ (**6**+**1a**), $[Ni_7(OH)_5(C_5H_9O_2)_9(C_5H_{10}O_2)_2(L^2)_2(H_2O)]\cdot H_2O$ (**6**+**1b**), $[Ni_7(OH)_5(C_5H_9O_2)_9(C_5H_{10}O_2)_2(L^3)_2(H_2O)]\cdot H_2O$ (**6**+**1c**), $[Ni_6(OH)_3(C_5H_9O_2)_9(C_5H_{10}O_2)_4(L^4)]\cdot 1.5C_6H_{14}$ (**6**′′), and $[Ni_4(OH)_3(C_5H_9O_2)_5(C_5H_{10}O_2)_4(L^5)]\cdot 1.5C_7H_8$ (**4**). Their structures were also determined by X-ray crystallography. Although Ni(II) trimethylacetates may have varying nuclearity and can change their nuclearity during recrystallization or interactions with nitroxides, this family of compounds is easy to study because of its topological relationship. For any of these complexes, the polynuclear framework may be derived from the [Ni6] polynuclear fragment $\{Ni_6(\mu_4\text{-}OH)_2(\mu_3\text{-}OH)_2(\mu_2\text{-}C_5H_9O_2\text{–}O,O')_6(\mu_2\text{-}C_5H_9O_2\text{–}O,O)(\mu_4\text{-}C_5H_9O_2\text{–}O,O,O',O')(C_5H_{10}O_2)_4\}$, which is shaped like an open book. On the basis of this fragment, the structure of 7-nuclear compounds (**7** and **6**+**1a**–**c**) is conveniently represented as the result of symmetric addition of other mononuclear fragments to the four Ni(II) ions lying at the vertexes of the [Ni6] open book. The 9-nuclear complex is formed by the addition of trinuclear fragments to two Ni(II) ions lying on one of the lateral edges of the [Ni6] open book. This wing of the 9-nuclear complex preserves its structure in another type of 6-nuclear complex (**6**′′) with the boat configuration. If, however, two edge-sharing Ni(II) ions are removed from [Ni6] (one of these lies at a vertex of the open book and the other, on the book-cover line), we obtain a 4-nuclear fragment recorded in the molecular structure of **4**. Twinning of this 4-nuclear fragment forms highly symmetric molecule **8**, which is a new chemical version of cubane.

Introduction

Trimethylacetate anions ($C_5H_9O_2$) have attracted increased interest as ligands that ensure a good solubility of their transition metal complexes in organic solvents. These complexes hold much promise as components of homogeneous catalytic hydrocarbon-oxidizing systems or as parent matrixes for metal transport on the surface of supports.[1,2] Reactions of polynuclear compounds of metals with organic paramagnets can also initiate the self-assembly of highly dimensional magnetoactive heterospin structures. Thus, a family of heterospin compounds, including those capable of cooperative magnetic ordering, was previously isolated from

* To whom correspondence should be addressed. E-mail: Victor.Ovcharenko@tomo.nsc.ru.
† International Tomography Center, Russian Academy of Sciences.
‡ Novosibirsk State University.
§ Institute of General and Inorganic Chemistry, Russian Academy of Sciences.

(1) (a) Çelenligil-Çetin, R.; Staples, R. J.; Stavropoulos, P. *Inorg. Chem.* **2000**, *39*, 5838. (b) Barton, D. H. R.; Doller, D. *Acc. Chem. Res.* **1992**, *25*, 504.
(2) Eremenko, I. L.; Nefedov, S. E.; Sidorov, A. A.; Golubnichaya, M. A.; Danilov, P. V.; Ikorskii, V. N.; Shvedenkov, Y. G.; Novotortsev, V. M.; Moiseev, I. I. *Inorg. Chem.* **1999**, *38*, 3764.

10.1021/ic0522028 CCC: $33.50
Published on Web 06/14/2006

mixtures of products obtained by reactions of $[Mn_6(O)_2(C_5H_9O_2)_{10}(THF)_4]$ with nitronyl nitroxides containing alkyl or heterocyclic substituents in the side chain.[3,4] Effective interaction between nitronyl nitroxide and polynuclear compound here was again promoted by a good solubility of the latter in low-polarity organic solvents. Therefore, our attention was attracted by nonanuclear Ni(II) trimethylacetate, which possesses a high solubility in hexane.[5] Indeed, our study resulted in the isolation of the first heterospin compounds based on polynuclear Ni(II) trimethylacetates and nitronyl nitroxides (L^1−L^5).

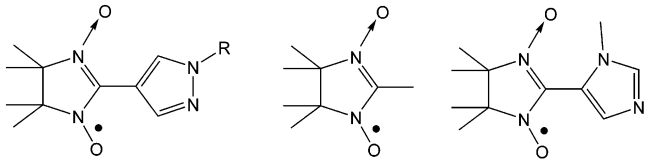

Other previously unknown polynuclear compounds of Ni(II) trimethylacetate isolated from hexane solutions in this study include $[Ni_6(OH)_4(C_5H_9O_2)_8(C_5H_{10}O_2)_4]$, $[Ni_7(OH)_7(C_5H_9O_2)_7(C_5H_{10}O_2)_6(H_2O)]\cdot 0.5C_6H_{14}\cdot 0.5H_2O$, and $[Ni_8(OH)_4(H_2O)_2(C_5H_9O_2)_{12}]$. This result is of independent value. The hexanuclear complex is an extremely important member of this series. Its structural fragment, $\{Ni_6(\mu_4\text{-}OH)_2(\mu_3\text{-}OH)_2(\mu_2\text{-}C_5H_9O_2{-}O,O')_6(\mu_2\text{-}C_5H_9O_2{-}O,O)(\mu_4\text{-}C_5H_9O_2{-}O,O,O',O')(C_5H_{10}O_2)_4\}$, can serve as a basis for constructing complex molecules other than hexanuclear. Of special interest is the highly symmetric $[Ni_8(OH)_4(H_2O)_2(C_5H_9O_2)_{12}]$, in which nickel atoms occupy all eight vertexes of its cube, an O atom of the hydroxo group or water molecule lies over the center of each of the six faces, and its 12 edges are linked by 12 μ_2-bridging (O,O′) trimethylacetate anions. Note that the CSD[6] contains no data about transition metal carboxylates with related structures. Therefore, $[Ni_8(OH)_4(H_2O)_2(C_5H_9O_2)_{12}]$ is believed to be another chemical version of a member of the cubane family.

Recently, Winpenny and co-workers reported on systematic topology of cobalt trimethylacetate cages. It was stressed that "one of the great challenges in polynuclear coordination chemistry is to establish reliable synthetic routes to oligomeric structures. Frequently complexes appear as isolated examples of a structural motif, and there seems to be no relationship between the polynuclear cage and the substrate used to synthesize this cage."[7] In this context, we feel it important to emphasize that our analysis of structural data for the above compounds has made it possible to reveal a topological relationship within the family of polynuclear nickel trimethylacetates. In recent years, transition metal carboxylate complexes have attracted attention because of the diversity of their structures and the similarity of their metal fragments to those in metal-containing enzymes.[8] In light of these findings, the topological relationship between the compounds discussed below may prove useful for studies of polynuclear nickel-containing fragments in enzymes and proteins.[8f]

Scheme 1

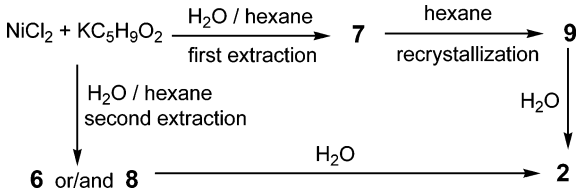

Results and Discussion

Synthesis. The reaction between the concentrated aqueous solutions of nickel chloride and potassium trimethylacetate was found to occur in a rather unusual manner. Stirring a mixture of these solutions is accompanied by a fast accumulation of the product suspended throughout the entire volume of the solution. Nontrivially, the reaction mixture completely consolidated at a definite moment of time. After a short interval (30−50 s), however, the resulting dry powder spontaneously started to release water; in 2 or 3 min, a two-phase system formed with a bright green transparent layer of mother solution clearly discernible over the fine precipitate. Treatment of the two-phase system with hexane (Scheme 1) led to large crystals of heptanuclear $[Ni_7(OH)_7(C_5H_9O_2)_7(C_5H_{10}O_2)_6(H_2O)]\cdot 0.5C_6H_{14}\cdot 0.5H_2O$ (**7**), growing (with high yield) from the water-saturated organic phase. Importantly, the organic extract does not need to be kept over the drying agent, because recrystallization of **7** from dry hexane leads to crystals of nonanuclear $[Ni_9(OH)_6(C_5H_9O_2)_{12}(C_5H_{10}O_2)_4]\cdot C_5H_{10}O_2\cdot 3H_2O$ (**9**) in good yield. Here and throughout, the numbers of the complexes match their nuclearity.

Resulting compounds **7** and **9** are the major products of synthesis. Repeated syntheses under varied synthetic conditions for **7** demonstrated the following. If, after the first extraction, the water residue is again treated with hexane (Scheme 1) and the extract decanted into an open flask, a film of intergrown fine crystals (which can occasionally be split into single crystals) forms on the walls of the flask in a few days. X-ray diffraction analysis showed that these crystals fit the formulas $[Ni_6(OH)_4(C_5H_9O_2)_8(C_5H_{10}O_2)_4]$ (**6**) and/or $[Ni_8(OH)_4(H_2O)_2(C_5H_9O_2)_{12}]$ (**8**). Single crystals **6** and/

(3) Ovcharenko, V.; Fursova, E.; Romanenko, G.; Ikorskii, V. *Inorg. Chem.* **2004**, 43, 3332.
(4) Fursova, E.; Ovcharenko, V.; Nosova, K.; Romanenko, G.; Ikorskii, V. *Polyhedron* **2005**, *24*, 2084.
(5) Eremenko, I. L.; Golubnichaya, M. A.; Nefedov, S. E.; Sidorov, A. A.; Golovaneva, I. F.; Burkov, V I.; Ellert, O. G.; Novotortsev, V. M.; Eremenko, L. T.; Sousa, A.; Bermejo, M. R. *Russ. Chem. Bull.* **1998**, *47*, 704.
(6) *Cambridge Structural Database*, version 5.26; Cambridge Crystallographic Data Centre: Cambridge, U.K., Nov 2004 (updates Aug 2005).
(7) Aromí, G.; Batsanov, A. S.; Christian, P.; Helliwell, M.; Parkin, A.; Parsons, S.; Smith, A. A.; Timco, G. A.; Winpenny, R. E. P. *Chem.—Eur. J.* **2003**, *9*, 5142.
(8) (a) Holm, H.; Kennepohl, P.; Solomon, E. I. *Chem. Rev.* **1996**, *96*, 2239. (b) Pearson, M. A.; Schaller, R. A.; Michel, L. O.; Karplus, P. A.; Hausinger, R. P. *Biochemistry* **1998**, *37*, 6214. (c) Lippard, S. J. *Science* **1995**, *268*, 996. (d) Karplus, P. A.; Pearson, M. A.; Hausinger, R. P. *Acc. Chem. Res.* **1997**, *30*, 330. (e) Ermler, U.; Grabarse, W.; Shima, S.; Goubeaud, M.; Thauer, R. K. *Science* **1997**, *278*, 1457. (f) *Handbook of Metalloproteins*; Messerschmidt, A., Huber, R., Poulos, T., Wieghardt, K., Eds.; John Wiley & Sons: New York, 2001; Vol. 2, pp 865−938.

Scheme 2. Topology of Framework Transformation in Polynuclear Nickel Trimethylacetates and Their Nitronyl Nitroxide Complexes[a]

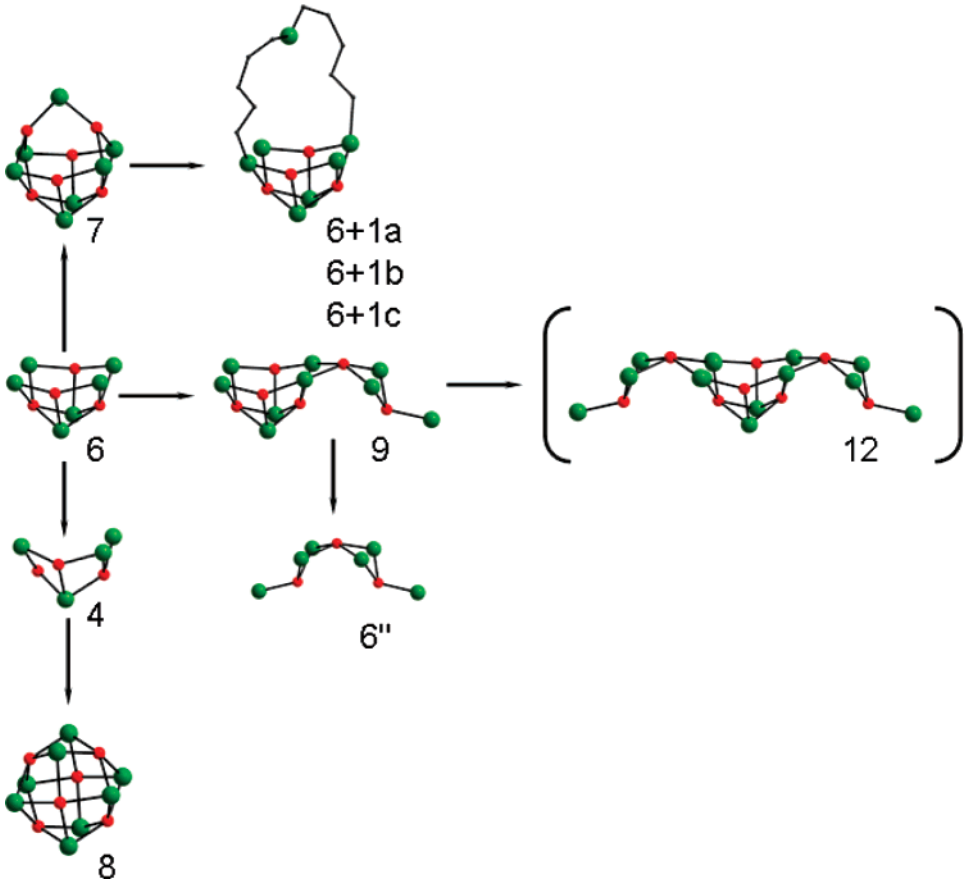

[a] The figures correspond to the nuclearity of the compounds and numbering of the complexes.

or **8** were too small and imperfect. Both were pale green plates, but crystals **6** were thin squares, whereas **8** were elongated thin rhombs. Attempts to grow more-perfect single crystals **6** or **8** in larger amounts via prolonged storage of these solutions always ended in the formation of perfectly faceted crystals of known binuclear complex $[Ni_2(C_5H_9O_2)_4(C_5H_{10}O_2)_4(H_2O)]$ (**2**).[9] The formation of **2** was significantly promoted by placing a few drops of excess water under the layer of the first or second hexane extract. Another observation was as follows. If, after the first extraction, the mother solution was separated from the bulk of crystals **7** and allowed to slowly evaporate, the flask walls sometimes also became covered with crystals **8** along with additional amounts of crystals **7** and **2**. Compound **8**, however, could not always be identified or separated as single crystals, and the crystals were much less perfect than crystals **8** obtained by slow evaporation of the second extract. Anyhow, prolonged storage (for one or more weeks) of the first or second extracts (after the third extraction, the amount of the product passing to the organic phase was negligibly small) ended in the formation of only hydrolysis product **2**. This suggests that the hexane extracts contained a rather complex mixture of the oligomer forms of Ni(II) trimethylacetate. We were unable to find any procedures for the preparation of individual **6** and **8** in large amounts. However, the occasional separability of single crystals **6** and **8** and their structure determination permitted us to derive a consistent structural topology of polynuclear Ni(II) trimethylacetates and their nitroxide complexes.

The structure and composition of the nitronyl nitroxide complexes of polynuclear Ni(II) trimethylacetates were dictated by the structure of the donor fragments of the paramagnetic L^1-L^5. All pyrazole-containing nitroxides L^1-L^3 formed heptanuclear molecules $[Ni_7(OH)_5(C_5H_9O_2)_9(C_5H_{10}O_2)_2(L^1)_2(H_2O)]\cdot 0.5C_6H_{14}\cdot H_2O$ (**6**+**1a**), $[Ni_7(OH)_5(C_5H_9O_2)_9(C_5H_{10}O_2)_2(L^2)_2(H_2O)]\cdot H_2O$ (**6**+**1b**), and $[Ni_7(OH)_5(C_5H_9O_2)_9(C_5H_{10}O_2)_2(L^3)_2(H_2O)]\cdot H_2O$ (**6**+**1c**), which belong to the same type regardless of which of the two polynuclear trimethylacetates (**7** or **9**) was used as a starting reagent. In Scheme 2 below, these heptanuclear compounds are designated by 6+1 because one of the nickel atoms in the molecule is far away from the polynuclear framework. Like **6**+**1a**−**c**, tetranuclear $[Ni_4(OH)_3(C_5H_9O_2)_5(C_5H_{10}O_2)_4(L^5)]\cdot 1.5C_7H_8$ (**4**) formed in good yield, resulting from the reaction of spin-labeled imidazole L^5 with **7** or **9**. Thin pale brown plates grew in small amounts on the flask walls during slow evaporation of solutions of Ni(II) trimethylacetate with L^4 in a CH_2Cl_2−hexane mixture. Some of these plates were occasionally separable. The structure and composition of

(9) (a) Mikhailova, T. B.; Fomina, I. G.; Sidorov, A. A.; Golovaneva, I. F.; Aleksandrov, G. G.; Novotortsev, V. M.; Ikorskii, V. N.; Eremenko, I. L. *Russ. J. Inorg. Chem.* **2003**, *48*, 1505. (b) Chaboussant, G.; Basler, R.; Gudel, H.-U.; Ochsenbein, S. T.; Parkin, A.; Parsons, S.; Rajaraman, G.; Sieber, A.; Smith, A. A.; Timco, G. A.; Winpenny, R. E. P. *Dalton Trans.* **2004**, 2758.

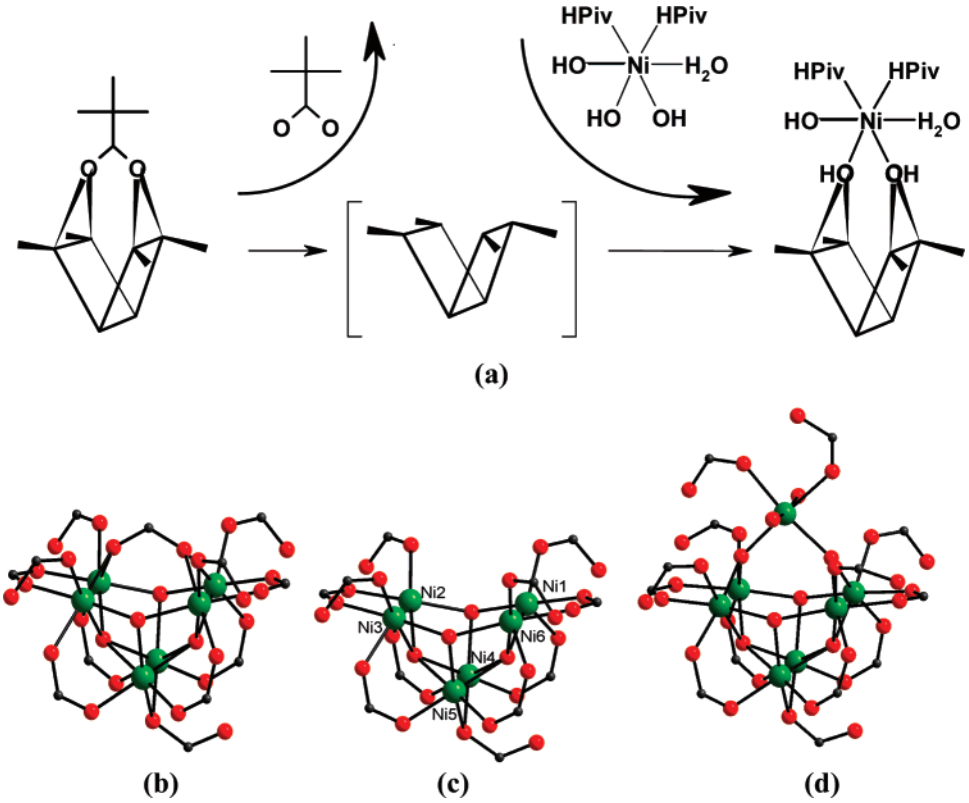

Figure 1. (a) Scheme of the transformation of **6** into **7**. (b) Hexanuclear molecule **6**. (c) Truncated fragment of the structure of compound **6**. (d) Heptanuclear molecule **7** (Ni, green ball; O, red ball; C, black ball). The $(CH_3)_3C$ groups are omitted for clarity.

$[Ni_6(OH)_3(C_5H_9O_2)_9(C_5H_{10}O_2)_4(L^4)]\cdot 1.5C_6H_{14}$ (**6″**) were determined by X-ray analysis.

Structure. To discuss the structure of the products we proceed from the general topological scheme (Scheme 2). In Scheme 2, the key complex is **6**; its metal core may be regarded as having an open book structure, or it may be viewed as being a trihedral prism if the vertexes of the open book are connected.

Figure 1a shows the formal route from **6** into **7**. Figure 1b depicts the basic structure-forming fragment $\{Ni_6(\mu_4\text{-}OH)_2(\mu_3\text{-}OH)_2(\mu_2\text{-}C_5H_9O_2{-}O,O')_6(\mu_2\text{-}C_5H_9O_2{-}O,O)(\mu_4\text{-}C_5H_9O_2{-}O,O,O',O')(C_5H_{10}O_2)_4\}$, whose *tert*-butyl groups are omitted for clarity. Six Ni atoms form a trigonal prism distorted along one of the vertical edges (Ni4−Ni5 in Figure 1c) bridged by the single anion (μ_2-$C_5H_9O_2$−O,O) of the structure. Over the planes of two tetragonal faces of the prism (Ni2, Ni3, Ni4, Ni5 and Ni1, Ni4, Ni5, Ni6 edges) are μ_4-OH groups ($d_{Ni-O} \approx 2.11-2.13$ Å). Two μ_3-OH groups ($d_{Ni-O} \approx 2.00-2.03$ Å) lie over the trigonal faces (Ni1, Ni2, Ni4 and Ni3, Ni5, Ni6 edges) of the imaginary prism.

The Ni···Ni distances along the tetragonal faces in the prism are different. The shortest Ni4−Ni5 edge is 2.70 Å, whereas the Ni2−Ni3 and Ni1−Ni6 edges are 3.05 and 3.04 Å, respectively. In the trigonal faces, the Ni3−Ni5 and Ni2−Ni4 (2.96 Å) distances are similar to those of Ni1−Ni4 and Ni5−Ni6 (2.94 Å). They are much shorter than the Ni1−Ni2 and Ni3−Ni6 distances (3.72 Å). Therefore, the prism may be viewed as having an open book (shown in Scheme 2) structure whose vertexes (Ni1, Ni2, Ni3, Ni6) are bridged by the tetradentate (μ_4-$C_5H_9O_2$−O,O,O′,O′) anion (d_{Ni-O} = 2.148 and 2.138 Å).

The other trimethylacetate coordination compounds may be divided into two types. The first six of these perform the bridging bidentate function (μ_2-$C_5H_9O_2$−O,O′). They are bridging the edges of the prism Ni1−Ni6, Ni2−Ni3, Ni1−Ni4, Ni5−Ni6, Ni2−Ni4, and Ni3−Ni5. All Ni−O distances in this group are from 1.981 to 2.065 Å. The other four trimethylacetates are monodentate compounds with Ni1, Ni2, Ni3, and Ni6 as the central atoms (d_{Ni-O} = 2.107 and 2.111 Å). Note that in formula **6**, $[Ni_6(OH)_4(C_5H_9O_2)_8(C_5H_{10}O_2)_4]$, the four trimethylacetates are protonated; i.e., they are regarded (on the basis of the electroneutrality principle and structural data) as being neutral trimethylacetic acid molecules. For these monodentate molecules, the C−O distances are quite different. The coordinated fragments may essentially be regarded as being double-bond components (C═O) because they are markedly shorter (1.233 and 1.237 Å) than the other C−O bonds in these molecules (1.318 and 1.321 Å).[10] For this reason, the latter may be logically linked with the (C−OH) fragments of the carboxyl groups.

Figure 1c shows a truncated fragment of molecule **6** stripped of its top μ_4-$C_5H_9O_2$−O,O,O′,O′ anion that bridges Ni1, Ni2, Ni3, and Ni6. From Figure 1 (a, d) it can be seen that the formation of **7** occurs via formal replacement of the above fragment by the hydroxoaquatrimethylacetate complex of Ni. Two OH groups of the complex species are coordi-

(10) Batsanov, A. S.; Struchkov, Y. T.; Timco, G. A.; Gerbeleu, N. V.; Manole, O. S.; Grebenko, S. V. *Russ. Coord. Chem.* **1994**, 712.

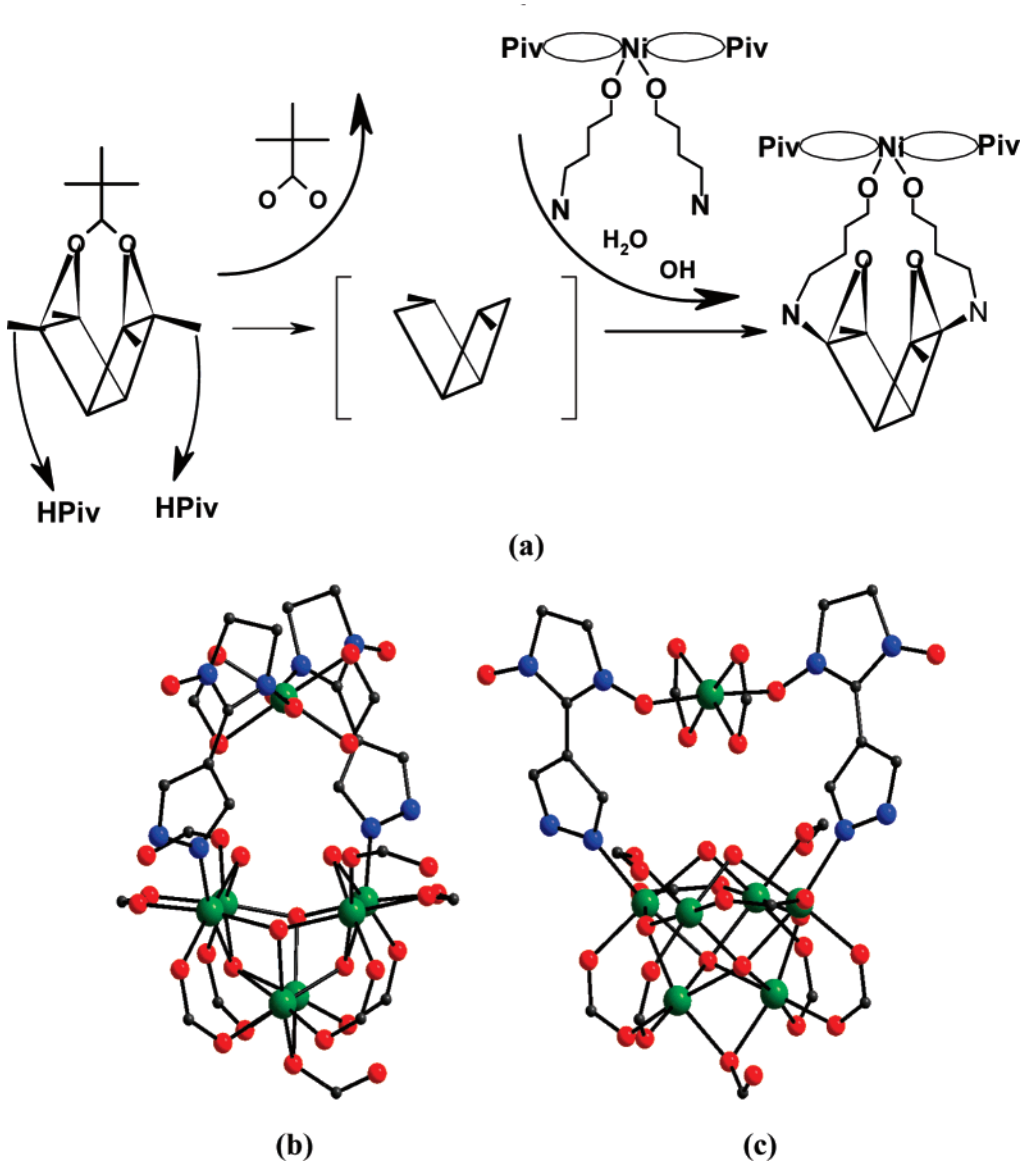

Figure 2. (a) Schematic drawing of the transformation of **6** into **6**+**1a**−**c**. (b, c) Two projections of heptanuclear molecule **6**+**1a**−**c**. (Ni, green ball; O, red ball; C, black ball; N, blue ball). The $(CH_3)_3C$ groups of trimethylacetates, the CH_3 groups of the imidazoline cycles, and the alkyl substituents at the pyrazole cycles (*i*-C_3H_7, *n*-C_4H_9, or *n*-C_6H_{13}) of L^1−L^3 are omitted for clarity.

nated by the Ni1, Ni2 and Ni3, Ni6 atoms, respectively. As a result, the hexanuclear fragment (Figure 1b) is completed to a heptanuclear one (Figure 1d), forming two more fragments with μ_3-bridging OH groups (top of Figure 1d). The suggested scheme of replacement is formal. However, it demonstrates an important point: on passing from **6** to **7**, the hexanuclear $\{Ni_6(\mu_4\text{-}OH)_2(\mu_3\text{-}OH)_2(\mu_2\text{-}C_5H_9O_2\text{−}O,O')_6\text{-}(\mu_2\text{-}C_5H_9O_2\text{−}O,O)(C_5H_{10}O_2)_4\}$ fragment remains unchanged.

Now, it would be appropriate to consider the topological scheme that outlines the formation of structurally related polynuclear complexes **6**+**1a**−**c** with spin-labeled pyrazoles (Figure 2). In Scheme 2, these complexes are denoted as **6**+**1** to show that one of the Ni atoms in the heptanuclear molecule is slightly detached from the hexanuclear framework, lying in a more remote position. The route leading from **6** to **6**+**1a**−**c** may be represented as follows. As in the previous case (Figure 1a), the μ_4-$C_5H_9O_2$−O,O,O′,O′ anion should be removed from the hexanuclear molecule to fulfill the transition depicted in panels b and c of Figure 1. The two monodentate trimethylacetic acid molecules diagonal to each other (i.e., at the Ni1 and Ni3 or Ni2 and Ni6 atoms, Figure 1c) should also be eliminated. Then only two ▲ symbols that denote the monodentate trtimethylacetic acid molecules would remain at the vertexes of the open book (in square brackets in Figure 2a). If the paramagnetic ligands (L^1−L^3) bonded to the additional Ni atom are now attached by their N donor atoms to the molecule and the OH and water oxygen atoms are placed instead of the oxygen atoms of μ_4-$C_5H_9O_2$−O,O,O′,O′, we obtain molecule **6**+**1a**−**c** (Figure 2a). As mentioned above, the hydrogen atoms were not localized in difference syntheses; therefore, the choice of the H_2O molecule and OH group was merely dictated by the electroneutrality principle. In panels b and c of Figure 2, the same molecule of the complex is given in different projections to reveal the similarity between the hexanuclear frameworks in **7** (Figure 1d), **6** (Figure 1b), and **6**+**1a**−**c**

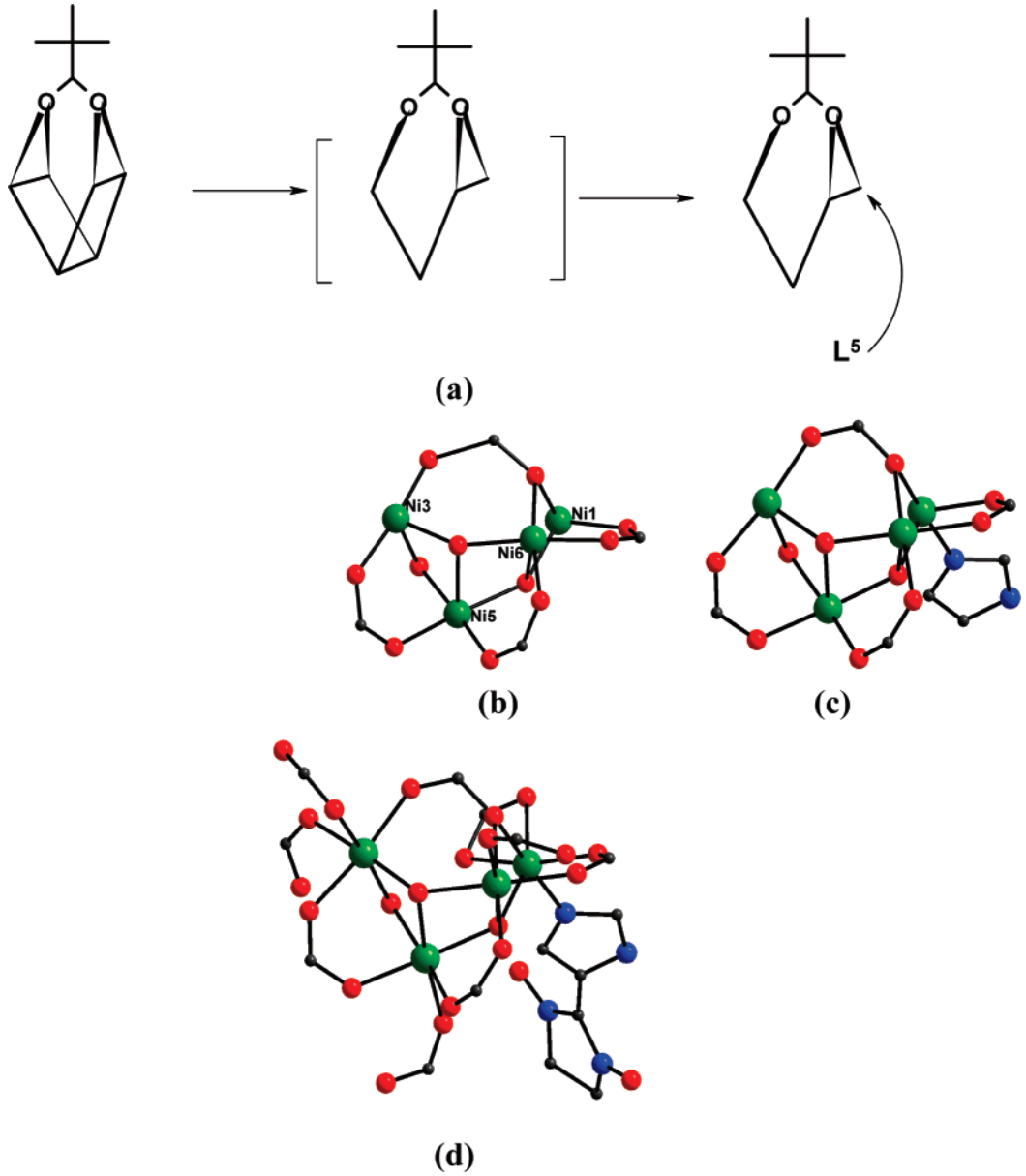

Figure 3. (a) Schematic drawing of the transformation of **6** into **4**. (b, c) Resemblance between the truncated tetranuclear fragments of **6** and **4**. (d) Tetranuclear molecule **4**. (Ni, green ball; O, red ball; C, black ball; N, blue ball). The $(CH_3)_3C$ groups of trimethylacetates and CH_3 substituents in the imidazoline and imidazole cycles of L^5 are omitted for clarity.

(Figure 2b) and to demonstrate the octahedral surroundings of the "extra" Ni atom that involve two bidentate trimethylacetates and the O atoms of the >N−O fragments of nitronyl nitroxides (Figure 2c). As a result, the Ni atom serves as a link to close the 18-membered ring (if the atoms are enumerated along the smallest perimeter). For easy perception of the molecular structure of **6**+**1a**−**c** in panels b and c of Figure 2, we have omitted the *tert*-butyl groups of trimethylacetates, as well as the methyl groups in the 2-imidazolidine ring and the alkyl substituents (*i*-C_3H_7, *n*-C_4H_9, or *n*-C_6H_{13}) at the loose N atoms of the L^1−L^3 pyrazole cycles. Thus, the suggested layout of the transformation of **6** into **6**+**1a**−**c** indicates that the $\{Ni_6(\mu_4\text{-}OH)_2(\mu_3\text{-}OH)_2(\mu_2\text{-}C_5H_9O_2{-}O,O')_6(\mu_2\text{-}C_5H_9O_2{-}O,O)(C_5H_{10}O_2)_2\}$ polynuclear fragment remains the same in both **6** and **6**+**1a**−**c**.

Figure 3a presents a topological scheme of the rearrangement of **6** into **4**. Even with *tert*-butyl groups removed from the molecule and with methyl groups taken away from the imidazoline and imidazole rings, molecule **4** (Figure 3d) is still too cumbersome to be viewed as an entity. Therefore, in Figure 3b, we left only the tetranuclear fragment, which is readily derived from the hexanuclear molecule (Figure 1b) by removing two Ni atoms (in Figure 1c, Ni2 and Ni4 are the atoms to be removed) and all monodentate trimethylacetic acid molecules. As a result, the tetranuclear framework that remained in molecule **6** is totally identical to the framework in the structure of **4**, presented in the same truncated form in Figure 3c. A comparison of the topological scheme (Figure 3a) with the truncated fragment (Figure 3c) clearly shows that nitroxide L^5 is coordinated by the metal atom designated as Ni1. To ensure a unified representation, all tetranuclear

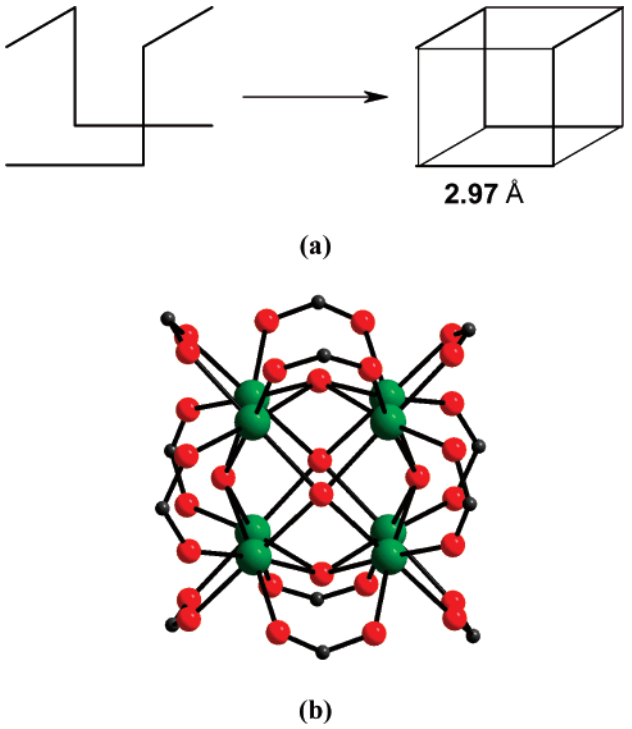

Figure 4. (a) Schematic drawing showing the formation of **8**. (b) Octanuclear molecule **8**. (Ni, green ball; O, red ball; C, black ball). The $(CH_3)_3C$ groups of trimethylacetates are omitted for clarity.

fragments in Figure 3 are orientated in such a way that the upper part should bear the single anion of the structure, μ_3-$C_5H_9O_2$−O,O,O′.

The topological scheme of a polynuclear framework was completed to the octanuclear level because of the presence of a tetranuclear fragment in molecule **4** that was obtained as the major product in the reaction of spin-labeled L^5 with **7** or **9** (Scheme 2). An octanuclear cubelike structure can evidently be readily derived topologically by consolidating two tetranuclear fragments, as shown in Figure 4a. Figure 4b presents the view of a real molecule of **8** with all *tert*-butyl fragments omitted for clarity. All eight of the cube vertexes are occupied by the Ni atoms. Each of the six faces has an O atom of the hydroxo group or water molecule above its center, and the 12 edges are bridged by 12 bridging bidentate trimethylacetates. All Ni−Ni distances in the molecule are identical (2.97 Å) within experimental error (Figure 4a). The C−O distances in the trimethylacetate ligands (1.193, 1.172, 1.156, 1.038 Å), the Ni−O_{OCO} distances (1.962, 1.945, 1.925, 1.916 Å), and the distances from the Ni atoms to the O atoms over the centers of the faces (2.088, 2.066, 2.062, 2.047 Å) are also identical. The lack of data about transition metal carboxylates with related structures in the CSD[6] gives us grounds to believe that **8** is another chemical version of a member of the cubane family. The closest structural relative of cubane **8** is probably the rhombohedral mixed-metal and mixed-ligand complex $[(NaCl)_2Ni_6(OH)_6(C_5H_9O_2)_6L_6]\cdot 4THF$ (L is 6-methyl-2-pyridonate) with two Na atoms replaced for Ni atoms on the body diagonal.[11]

The molecular structure of **9** is shown in Figure 5a. We shall not discuss it here in detail because a similar structure was described elsewhere,[5] where the nonanuclear complex was investigated as solvate crystals with four water molecules, a trimethylacetic acid half-molecule, and a benzene half-molecule. In our study, this complex was synthesized and investigated as a solvate with three water molecules and one trimethylacetic acid molecule readily obtained in good yield by recrystallization of **7** from hexane (see Experimental Section). For purposes of our treatment, the only thing we need is the nonanuclear core of the complex (Figure 5a), which resembles the Big Dipper constellation. On the topological scheme (Scheme 2), this is complex **9**. The prismatic fragment of **6** (panels b and c of Figure 1) is obviously fully coincident with the same fragment of **9** (Figure 5) (in Figure 5b, we intentionally enumerated the Ni1−Ni6 atoms in the prism in the same way as in Figure 1c). The Ni2−Ni3 and Ni1−Ni6 edges of the prism (Figure 1c) being structurally indistinct, further construction of the polynuclear framework might equally go "right" and "left," i.e., at the Ni2−Ni3 and Ni1−Ni6 edges. This could ultimately result in a dodecanuclear compound, whose topological scheme of the polynuclear metal core is given in square brackets in Scheme 2. Regretfully, no such compound has ever been recorded. In any batch of single crystals obtained by recrystallization of **7** from hexane, we always found compound **9** alone.

The method used to expand the hexanuclear prismatic framework by adding three Ni atoms (denoted as Ni7, Ni8, and Ni9 in Figure 5b) is important for understanding the structural topological relationship between **9** and hexanuclear complex **6″** containing the L^4 nitroxide. The molecular structure is shown in Figure 5c. It is represented by a symmetrically expanded fragment of Ni1, Ni6, Ni7, and Ni8 atoms (Figure 5b). If the framework is symmetrically complemented with Ni9 and Ni9′ (Figure 5d), we obtain a polynuclear fragment of molecule **6″**. In **9**, the Ni1, Ni6, Ni7, and Ni8 atoms in the bottom part of the "side" fragment link two bridging tridentate trimethylacetate ligands, whereas in **6″**, the same Ni atoms connect the O,O-bridging oxygen atoms of L^4 and trimethylacetate ligand. That is why in Scheme 2, hexanuclear compound **6″** is shown as a derivative of **9**. Note that the molecular structure of any nitronyl nitroxide does not markedly change after addition of the latter to a polynuclear heterospin complex. The distances in the NO group are from 1.251(9) to 1.310(6) Å; the longest of these is observed in **6″** with bridging L^4. The Ni−O_{NO} distances do not differ from the Ni−O_{OCO} distances to coordinated trimethylacetates.

Thus, our study indicated that all of the isolated complex molecules based on polynuclear nickel pivalates contain common structural fragments whose mutual transformations are summarized as a single topological scheme (Scheme 2).

Magnetic Properties. Analysis of the magnetic properties of Ni(II) polynuclear compounds is currently a rather complex problem.[12] Recently, the results of detailed magnetochemical and neutron diffraction studies of the tetra-

(11) Brechin, E. K.; Graham, A.; Harris, S. G.; Parsons, S.; Winpenny, R. E. P. *J. Chem. Soc., Dalton Trans.* **1997**, 3405.

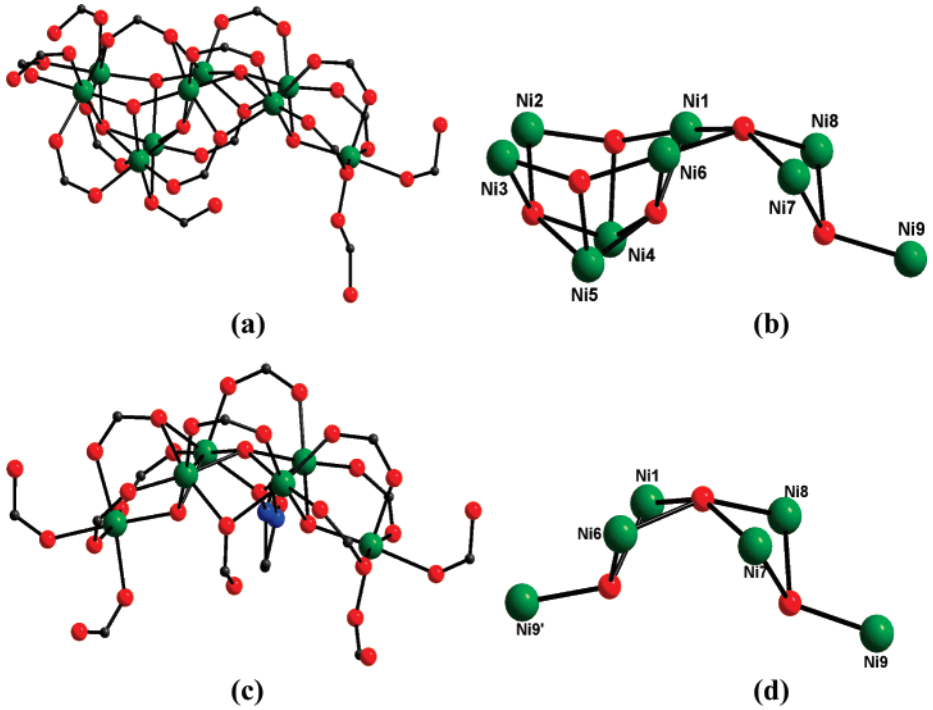

Figure 5. (a) Structure of molecule **9**. The $(CH_3)_3C$ groups of trimethylacetates are omitted for clarity. (Ni, green ball, O, red ball, C, black ball). (b) Nonanuclear frame of molecule **9**. (c) Structure of molecule **6″**, and (d) structure of **6″** with the $(CH_3)_3C$ groups of trimethylacetates and the CH_3 groups of the imidazoline cycle omitted for clarity. (Ni, green ball; O, red ball; C, black ball; N, blue ball).

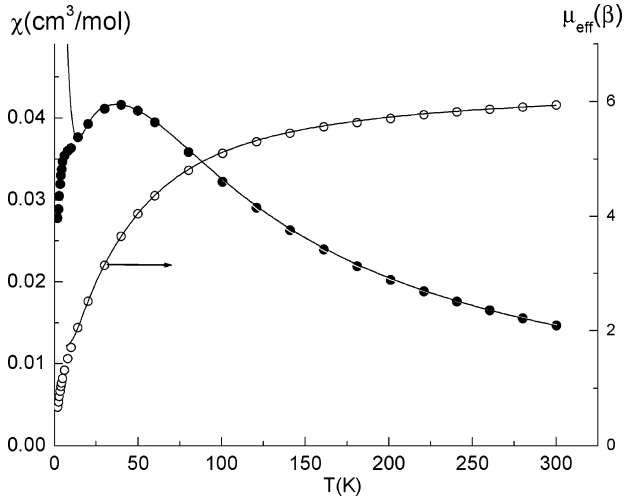

Figure 6. Temperature dependence of susceptibility (○) measured in an applied magnetic field of 5 kOe, and temperature dependence of the effective magnetic moment of **4** (●). Theoretical curves are the solid lines.

nuclear trimethylacetate complex $[Ni_4(\mu_3\text{-}OH)_2(O_2CCMe_3)_6(EtOH)_6]$ have been published.[12b] These data were employed to analyze the magnetic properties of our tetranuclear complex with L^5 nitroxide (Figure 3d). The effective magnetic moment (μ_{eff}) of **4** decreases monotonically from 5.93 β at 300 K to 0.67 β at 2 K (Figure 6), which indicates that antiferromagnetic exchange interactions dominate in the solid. The value of μ_{eff} at 300 K corresponds to the expected spin-only value (5.92 β) for four weakly interacting Ni(II) paramagnetic centers with $S = 1$ and one nitroxide with $S = 1/2$. Magnetic susceptibility (χ) as a function of temperature has a maximum at 40 K. Below 5 K, χ abruptly decreases.

On the basis of the structural data of **4**, the magnetic structure of the complex molecule may be represented as involving an exchange cluster formed from four Ni(II) ions and the radical's nitroxyl group weakly interacting with these ions (Figure 7a), with the intramolecular distance between the Ni1 atom and the nitroxyl N atom exceeding 6 Å. Figure 7b shows intramolecular short distances between the Ni atoms. In Figure 7b, the Ni atoms are numbered in the same way as in Figure 3d. All intermolecular distances between the paramagnetic centers are very long. The shortest among them are the distances between nitroxyl groups (4.827 Å) because in the solid, molecules **4** are packed in pairs in which the >N−O fragments of the nitroxyl groups face each other. Thus the scheme of exchange interactions is simplified to the scheme presented below.

To describe the temperature dependence of χ in the calculated model, we set $J_3 = 0$. With this assumption for tetranuclear cluster **4**, we may record the exchange spin Hamiltonian as follows

$$H = -2J_0S_1S_2 - 2J_1(S_1S_3 + S_2S_4) - 2J_2(S_1S_4 + S_2S_3) \quad (1)$$

The program and scheme of calculations for heterospin clusters used for optimization in determining the exchange parameters of Hamiltonian (1) is described elsewhere.[12c] The resulting theoretical curves (solid lines in Figure 6) correspond to the optimal parameters of the Hamiltonian: $J_0 = -1.7 \pm 0.2$ cm^{-1}, $J_1 = -18.4 \pm 0.3$ cm^{-1}, $J_2 = -1.1 \pm 0.1$

(12) (a) Kahn, O. *Molecular Magnetism*; VCH: New York, 1993. (b) Chaboussant, G.; Basler, R.; Güdel, H.-U.; Ochsenbein, S.; Parkin, A.; Parsons, S.; Rajaraman, G.; Sieber, A.; Smith, A. A.; Timco, G. A.; Winpenny, R. E. P. *Dalton Trans.* **2004**, 2758. (c) Ovcharenko, I. V.; Shvedenkov, Y. G.; Musin, R. N.; Ikorskii, V. N. *J. Struct. Chem.* **1999**, *40*, 29.

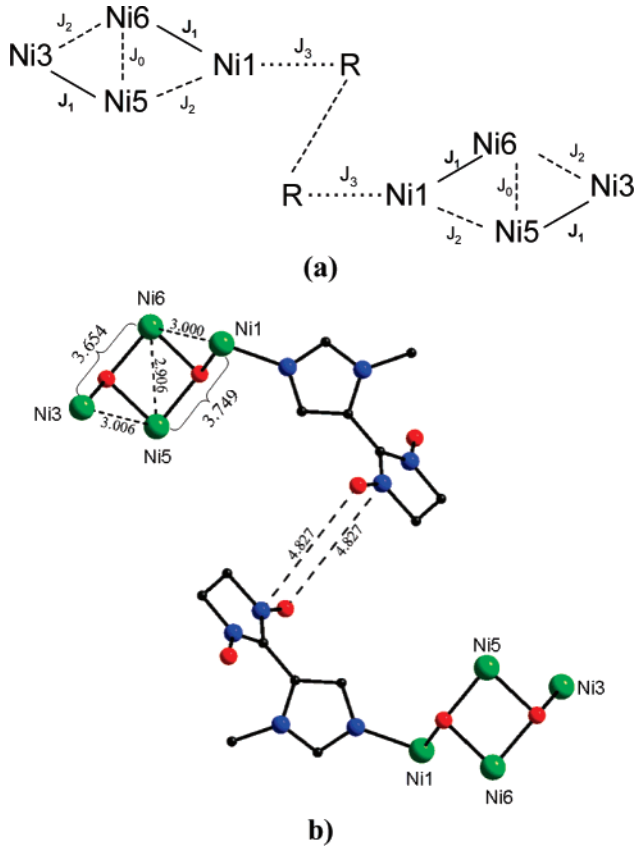

Figure 7. (a) Schematic representation of the magnetic exchange scheme in **4**; (b) corresponding fragment of the real structure.

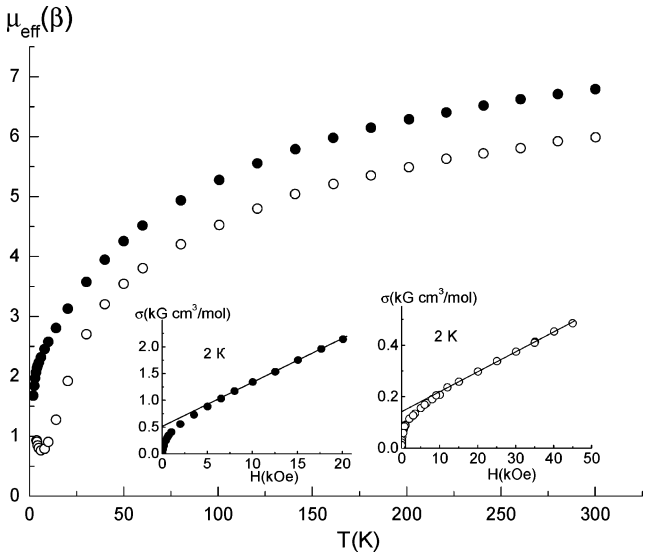

Figure 8. Temperature dependences of μ_{eff} for **7** (●) and **6**+**1b** (○). Inserts: field dependences of magnetization for **7** (●) and **6**+**1b** (○) measured at 2 K.

cm^{-1}, $g = 2.15 \pm 0.01$. The obtained values of the parameters J_0, J_1, and J_2 are very close to those for the previously described compound $[Ni_4(\mu_3\text{-}OH)_2(O_2CCMe_3)_6(EtOH)_6]$,[12b] with the same structure of the polynuclear fragment as that in **4**.

As can be seen in Figure 6, the theoretical curve fits the experimental data above 13 K well. Below this temperature, the theoretical and experimental curves diverge. The calculations neglected exchange interactions of odd electrons of nitroxyl groups within pairs of molecules separated by distances of 4.827 Å (Figure 7b). The sharp decrease in χ below 5 K is believed to be the result of antiferromagnetic exchange interactions within such pairs of nitroxyl fragments.

Figure 8 shows the results of our study of complexes **7** and **6**+**1b** (the latter is considered a typical representative of the series **6**+**1a**−**c**). As can be seen for both complexes, μ_{eff} decreases with temperature from 6.79 and 5.99 β at 300 K to 1.68 and 0.93 β at 2 K for **7** and **6**+**1b**, respectively. Because compound **7** has seven paramagnetic centers with $S = 1$, in the case of weak interactions between these centers, the theoretical spin-only value of the magnetic moment at elevated temperatures must be 7.48 β (for $g = 2$). At room temperature the experimental value is slightly lower, which indicates that antiferromagnetic exchange interactions play a pronounced role. The experimental dependence $\mu_{eff}(T)$ for **6**+**1b** is below that for **7**, although molecule **6**+**1b** formally has more paramagnetic centers. This is due to the fact that the spin of the remote quasi-isolated Ni(II) ion is completely compensated by the spins of two coordinated nitroxyl groups in the >N−•O−Ni(II)−O•−N< fragment (Figure 2c) with short distances $d_{Ni-O} = 2.049$ and 2.057 Å (Table 2). Therefore, the magnetic properties of **6**+**1b** are almost completely dictated by the remaining hexanuclear fragment of the molecule. For a system of six weakly interacting centers with $S = 1$, the theoretical spin-only value of μ_{eff} is 6.93 β, which the experimental dependence tends to at high temperatures.

The field dependences of magnetization (σ) at 2 K are given in the inserts of Figure 7 for both complexes. The curves of these dependences cannot be defined in terms of the Brillouin function and thus cannot be explained by saturation effects. They may be described in terms of the function $\sigma = \sigma_s + \chi H$, where σ_s is spontaneous magnetization. Spontaneous magnetization σ_s is 528 and 144 G cm^3/mol for **7** and **6**+**1b**, respectively. It is plausible that sources of magnetization are minor deviations from collinearity during antiferromagnetic ordering of magnetic moments within the polynuclear fragments, which are nearly identical in the two complexes.

Figure 9 shows the temperature dependence of μ_{eff} for complex **9**, whose molecule is a complex exchange-coupled system of nine Ni(II) ions (Figure 5b). The value of μ_{eff} for **9** is 8.5 β at room temperature, which agrees with the spin-only value of 8.49 β for nine weakly interacting paramagnetic centers with $S = 1$. The magnetic moment μ_{eff} has a minimum of 5.7 β at reduced temperatures and a maximum of 5.9 β at still-lower temperatures. The complex character of the temperature dependence of μ_{eff} is obviously the result of competition between numerous exchange-interaction channels in **9**. The field dependence of magnetization shown in the insert of Figure 9 is described in terms of the Brillouin function. From this curve, it can be seen that below 5000 Oe, at which the temperature dependence of μ_{eff} was measured, the magnetization curve remains linear.

Table 1. Crystal Data, Experimental Details, and Selected Bond Lengths (Å) for **6**−**9**

	6	**7**		**8**	**9**
formula	$C_{60}H_{116}Ni_6O_{28}$	$C_{68}H_{140}Ni_7O_{34.5}$		$C_{60}H_{114}Ni_8O_{30}$	$C_{85}H_{170}Ni_9O_4$
fw	1637.79	1920.77		1785.19	2408.60
T (K)	240	298	200	298	200
cryst syst	monoclinic	orthorhombic		rhombohedral	orthorhombic
space group	$P2_1/m$	$P2_12_12_1$		$R\bar{3}$	$Pnma$
a (Å)	13.825(2)	15.1272(8)	15.014(1)	21.967(9)	24.352(1)
b (Å)	23.858(3)	26.934(2)	26.636(2)		17.678(1)
c (Å)	14.466(2)	27.274(2)	26.912(2)	15.026(9)	29.779(2)
β	90.481(2)				
V (Å^3)	4771.5(12)	11112(1)	10763(1)	6279(5)	12820(1)
Z	2	4	4	3	4
D_{calcd} (g/cm^3)	1.114	1.148	1.185	1.416	1.248
μ (mm^{-1})	1.219	1.223	1.266	1.830	1.361
total no. of reflns/unique	20 625/7069	48 730/16038	47 051/15581	8972/1986	54 726/9587
R_{int}	0.0910	0.0593	0.675	0.2752	0.0659
θ_{max} (deg)	23.36	23.32	23.38	23.23	23.30
N	514	1138	1138	167	789
GOF	0.800	0.937	0.919	0.817	0.972
R_1	0.0644	0.0543	0.0491	0.0892	0.0622
wR_2 ($I > 2\sigma(I)$)	0.1905	0.1417	0.1293	0.1858	0.1888
R_1	0.0939	0.0691	0.0586	0.3487	0.0903
wR_2 (all data)	0.2143	0.1486	0.1343	0.2598	0.2090
Ni−Ni	2.6998(16)	2.700(1)	2.693(1)	2.794(4)	2.744(2)
	2.9383(12)	2.9489(9)	2.945(1)	2.791(4)	2.919(1)
		2.9565(10)	2.952(1)		2.722(2)
	2.9629(12)	2.9447(9)	2.938(1)		2.911(1)
		2.9514(9)	2.967(1)		2.826(2)
		2.9714(10)	2.942(1)		
		2.9525(9)	2.944(1)		
Ni−O	1.979(5)−2.187(4)	1.982(5)−2.187(3)		1.916(15)−2.088(8)	1.977(4)−2.178(4)

Conclusions

Thus, our study has revealed new polynuclear Ni(II) trimethylacetates whose high solubility in low polar organic solvents enabled us to perform their reactions with nitronyl nitroxides. For all polynuclear compounds of Ni(II) and their complexes with nitroxides isolated in this study, the molecular and crystal structure has been solved. Although Ni(II) trimethylacetates can form complexes of varying nuclearity and the latter can change during recrystallization or interactions with nitroxides, investigation of this family of compounds is considerably facilitated if they are treated within a single structural approach. It appeared that for all of these complexes, the polynuclear framework may be derived from the polynuclear fragment $\{Ni_6(\mu_4\text{-}OH)_2(\mu_3\text{-}OH)_2(\mu_2\text{-}C_5H_9O_2\text{−}O,O')_6(\mu_2\text{-}C_5H_9O_2\text{−}O,O)(\mu_4\text{-}C_5H_9O_2\text{−}O,O,O',O')\text{-}(C_5H_{10}O_2)_4\}$ (Figure 1b) that is shaped like an open book. The structure of the highly symmetric cubane molecule $[Ni_8\text{-}(OH)_4(H_2O)_2(C_5H_9O_2)_{12}]$ is also of interest (Figure 4b). Because the CSD[6] has no information about transition metal carboxylates with a similar structure, $[Ni_8(OH)_4(H_2O)_2\text{-}(C_5H_9O_2)_{12}]$ is believed to be a new member of the cubane family.

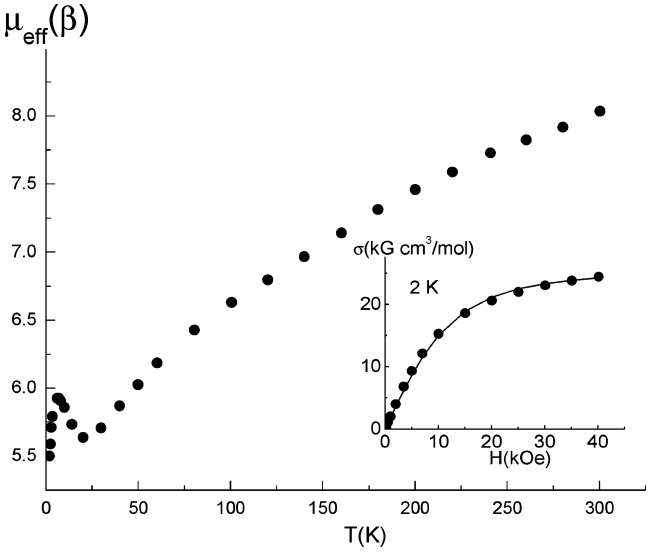

Figure 9. Temperature dependence of the effective magnetic moment of **9** measured in an applied magnetic field of 5 kOe. Insert: field dependence of magnetization for **9** measured at 2 K (the solid line is the Brillouin curve).

Experimental Section

General Methods. ^{1}H NMR spectra were recorded on a Bruker 300 NMR instrument at room temperature. The chemical shifts were reported as δ values in parts per million calibrated against the peaks of a protic solvent. IR spectra were recorded on a Bruker Vector 22 instrument for KBr pellets. The magnetic measurements were carried out on an MPMS-5S SQUID magnetometer (Quantum Design) in the temperature range 2−300 K in a magnetic field of up to 45 kOe. The molar magnetic susceptibility χ was calculated using Pascal's additive scheme with corrections for the diamagnetism of the compounds. The effective magnetic moment was calculated as $\mu_{eff} = (8\chi T)^{1/2}$. Silica gel 60 (0.063−0.200 mm) (Merck) was used for column chromatography. 2,3-Bis(hydroxylamino)-2,3-dimethylbutane monosulfate monohydrate[13] and 2,4,4,5,5-pentamethyl-4,5-dihydro-1*H*-imidazole-3-oxide-1-oxyl (L^4)[14] were synthesized according to known procedures.

1-Isopropyl-1*H*-pyrazole. A mixture of pyrazole (6.8 g, 0.1 mol) and KOH (6.16 g, 0.11 mol) was stirred in water (6 mL) for 30 min at room temperature. 2-Bromopropane (13.1 g, 0.11 mol) was

(13) Ovcharenko, V. I.; Fokin, S. V.; Romanenko, G. V.; Korobkov, I. V.; Rey, P. *Russ. Chem. Bull.* **1999**, *48*, 1519.
(14) Boocock, D. G. B.; Darcy, R.; Ullman, E. F. *J. Am. Chem. Soc.* **1968**, *90*, 5945.

Table 2. Crystal Data, Experimental Details, and Selected Bond Lengths (Å) for **4**, **6″**, **6**+**1a**−**c**

	4	**6″**	**6**+**1b**	**6**+**1a-I**	**6**+**1a-II**	**6**+**1c**
formula	$C_{66.5}H_{117}N_4Ni_4O_{23}$	$C_{82}H_{160}N_2Ni_6O_{31}$	$C_{83}H_{156}N_8Ni_7O_{33}$	$C_{84}H_{159}N_8Ni_7O_{33}$	$C_{84}H_{159}N_8Ni_7O_{33}$	$C_{87}H_{164}N_8Ni_7O_{33}$
fw	240	240	298	298	240	240
T (K)	1575.48	2022.38	2205.13	2220.16	2220.16	2261.23
cryst syst	triclinic	triclinic	monoclinic	triclinic	monoclinic	monoclinic
space group	$P\bar{1}$	$P\bar{1}$	$P2_1/c$	$P\bar{1}$	$P2_1/c$	$P2_1/n$
a (Å)	14.719(4)	14.183(3)	27.594(8)	15.760(1)	14.492(1)	15.2765(9)
b (Å)	16.350(4)	16.520(3)	16.176(5)	16.8560(1)	28.646(2)	28.221(2)
c (Å)	19.068(5)	26.826(5)	29.832(9)	22.310(1)	29.740(2)	29.126(2)
α	95.948(5)	104.476(4)		85.306(2)		
β	95.077(5)	90.556(5)	114.979(6)	89.459(2)	92.773(2)	102.757(1)
γ (deg)	102.827(6)	114.503(4)		80.446(2)		
V (Å^3)	4421.0(19)	5492.0(19)	12071(6)	5824.6(7)	12332(1)	12246.8(13)
Z	2	2	4	2	4	4
D_{calcd} (g/cm^3)	1.184	1.223	1.213	1.266	1.196	1.226
μ (mm^{-1})	0.902	1.075	1.136	1.177	1.112	1.121
total no. of reflns/unique	19 300/12 776	24 011/15 787	52 956/18 286	25 496/16 680	52 980/17 655	52 569/17 595
R_{int}	0.1261	0.0720	0.1615	0.0807	0.1488	0.0520
θ_{max} (deg)	23.44	23.40	23.94	23.64	23.28	23.33
N	973	1174	1344	1353	1356	1367
GOF	1.075	0.917	0.907	0.708	0.708	1.016
R_1	0.1141	0.0683	0.0826	0.0602	0.0606	0.0602
wR_2 ($I > 2\sigma(I)$)	0.2239	0.1372	0.1725	0.1145	0.1499	0.1690
R_1	0.1876	0.1233	0.1765	0.1529	0.1771	0.0878
wR_2 (all data)	0.2569	0.1550	0.2088	0.1443	0.1922	0.1821
Ni−Ni	2.907(2), 3.000(2), 3.006(2)	2.777(1), 2.776(1)	2.950(1), 2.963(1), 2.687(1), 2.931(1), 2.977(2)	2.686(1), 2.915(1), 2.981(1), 2.929(1), 2.977(1)	2.677(2), 2.923(2), 2.961(2), 2.982(2), 2.947(2)	2.680(1), 2.937(1), 2.929(1), 2.973(1), 2.954(1)
Ni−O	2.000(5)−2.148(6)	1.979(5)−2.184(4)	1.974(5)−2.210(5)	1.976(6)−2.197(5)	1.956(8)−2.149(5)	1.979(4)−2.204(3)
Ni−N	2.033(7)		2.128(6) 2.155(6)	2.169(6) 2.181(7)	2.152(8) 2.162(8)	2.147(5) 2.156(4)
Ni−O_L		2.084(5) 2.086(5)	2.057(5) 2.049(5)	2.048(5) 2.047(5)	2.040(6) 2.048(6)	2.054(4) 2.057(4)
N−O	1.254(9) 1.251(9)	1.310(6) 1.277(10)	1.267(7) 1.315(7) 1.288(8) 1.261(8)	1.299(7) 1.285(7) 1.278(8) 1.262(7)	1.292(8) 1.290(9) 1.247(10) 1.258(9)	1.294(5) 1.291(6) 1.290(6) 1.275(6)

added, and the resulting reaction mixture was boiled for 20 h. Then the mixture was filtered, and the filtrate was stirred with benzene. The organic layer was separated, dried over K_2CO_3, and filtered through Al_2O_3 (2 × 10 cm). The solvent was removed in a vacuum. The yellow oil product was twice distilled over KOH and then over metallic Na. Yield: 3.4 g (31%). Bp: 141−145 °C (lit.:[15] bp 137 °C (632 Torr)). ^{1}H NMR ($CDCl_3$): δ 1.56 (d, 6H, CH(CH_3)$_2$, J = 8.2 Hz), 4.04 (m, 1H, N−CH, J = 8.2 Hz), 6.21 (t, 1H, H(4), J = 2.1 Hz), 7.35 (d, 1H, H(3), $J_{3,4}$ = 2.2 Hz), 7.48 (d, 1H, H(5), $J_{4,5}$ = 1.9 Hz).

1-Butyl-1*H*-pyrazole. The synthetic procedure is similar to the one described above. The reaction was carried out in a minimal amount of water at 60 °C for 4 h. Yield: 90%. Bp: 176−178 °C, n_D^{20} 1.4671. ^{1}H NMR ($CDCl_3$): δ 0.92 (t, 3H, CH_3, J = 8.1 Hz), 1.30 (m, 2H, CH_2(3), J = 8.1 Hz), 1.83 (pentet, 2H, CH_2(2), J = 8.1 Hz), 4.11 (t, 2H, N−CH_2, J = 8.1 Hz), 6.21 (t, 1H, H(4), J = 2.1 Hz), 7.35 (d, 1H, H(3), $J_{3,4}$ = 2.2 Hz), 7.48 (d, 1H, H(5), $J_{4,5}$ = 1.9 Hz). Element analysis was fulfilled for the picric acid salt.

1-Butyl-1*H*-pyrazole Picrate. Picric acid (350 mg, 1.53 mmol) was added to 1-butyl-1*H*-pyrazole (200 mg, 1.61 mmol) in ethanol (2 mL). The reaction mixture was heated to boiling and then cooled. The precipitate was filtered off and recrystallized from a (5:1) mixture of benzene and hexane. Yield: 420 mg (78%). Mp: 69−70 °C. Anal. Calcd for $C_{13}H_{15}N_5O_7$ (mol wt = 353.29): C, 44.2; H, 4.3; N, 19.8. Found: C, 43.6; H, 4.0; N, 19.7.

1-Hexyl-1*H*-pyrazole. The procedure is similar to the one given for 1-isopropyl-1*H*-pyrazole. The reaction was conducted in a minimal amount of water at 70 °C for 3 h. Yield: 96%. Bp: 212−214 °C, n_D^{20} 1.4658. ^{1}H NMR ($CDCl_3$): δ 0.86 (t, 3H, CH_3, J = 8 Hz), 1.27−1.48 (m, 6H, $(CH_2)_3$), 1.83 (pentet, 2H, CH_2(2), J = 8 Hz), 4.11 (t, 2H, N−CH_2, J = 8 Hz), 6.21 (t, 1H, H(4), J = 2.1 Hz), 7.35 (d, 1H, H(3), $J_{3,4}$ = 2.2 Hz), 7.48 (d, 1H, H(5), $J_{4,5}$ = 1.9 Hz). Element analysis was fulfilled for the picric acid salt.

1-Hexyl-1*H*-pyrazole Picrate. Picric acid (200 mg, 0.87 mmol) was added to hexyl-1*H*-pyrazole (150 mg, 0.99 mmol) in ethanol (2 mL). Ethanol was removed from the solution with an air flow. The dry residue was recrystallized from a 1:5 mixture of benzene with hexane. Yield: 230 mg (70%). Mp: 74−75 °C. Anal. Calcd for $C_{15}H_{19}N_5O_7$ (mol wt = 381.35): C, 47.2; H, 5.0; N, 18.4. Found: C, 47.3; H, 4.8; N, 18.5.

1-Isopropyl-1*H*-pyrazole-4-carbaldehyde. The procedure is similar to the one described in the literature.[16] $POCl_3$ (6.14 g, 0.04 mol) was added dropwise with stirring at 130−135 °C to a solution of 1-isopropyl-1*H*-pyrazole (3.34 g, 0.03 mol) in DMF (10 mL). The reaction mixture was then stirred at 140−150 °C for 3 h. After the mixture was cooled, 40% aqueous NaOH was added dropwise to pH 9−10. The mixture was then diluted with water (50 mL) and transferred to a separating funnel. The organic layer was separated from the aqueous one, and the product was extracted with $CHCl_3$ (5 × 20 mL). The organic extracts were consolidated, dried with K_2CO_3, and filtered through an Al_2O_3 layer (2 × 10 cm). The solvent was removed in a vacuum. The dark brown residue was purified by vacuum distillation. Yield: 2.85 g (68%). Bp: 82−84 °C (2 Torr), n_D 1.5088.

(15) Vaughan, J. D.; Jewett, G. L.; Vaughan, V. L. *J. Am. Chem. Soc.* **1967**, *89*, 6218.

(16) Finar, J. L.; Lord, Q. H. *J. Chem. Soc.* **1957**, 3314.

1-Butyl-1*H*-pyrazole-4-carbaldehyde. The reaction of 1-butyl-1*H*-pyrazole (9.60 g, 0.077 mol) with DMF (30 mL) and $POCl_3$ (13.1 g, 0.085 mol) was carried out using a similar procedure. Yield: 2.6 g (22%). Bp: 100−102 °C (1 Torr). ^{1}H NMR ($CDCl_3$): δ 0.99 (t, 3H, CH_3, J = 8.1 Hz), 1.36 (m, 2H, CH_2(3), J = 8.1 Hz), 1.92 (pentet, 2H, CH_2(2), J = 8.1 Hz), 4.19 (t, 2H, N−CH_2, J = 8.1 Hz), 7.98 (s, 1H, H(3)), 8.01 (s, 1H, H(5)), 9.89 (s, 1H, CHO). Element analysis was performed for the corresponding dinitrophenylhydrazone. 1-Butyl-1*H*-pyrazole-4-carbaldehyde (160 mg, 1.05 mmol) and concentrated HCl (50 μL) were added to a boiling solution of dinitrophenylhydrazone (200 mg, 1.01 mmol) in ethanol (30 mL). The reaction mixture was boiled for 20 min. After the mixture was cooled, the residue was filtered off and recrystallized from a 1:1 mixture of benzene and hexane. Yield: 260 mg (78%). Mp: 188−189 °C. ^{1}H NMR ($CDCl_3$): δ 1.01 (t, 3H, CH_3, J = 8.1), 1.38 (m, 2H, CH_2(3), J = 8.1 Hz), 1.94 (pentet, 2H, CH_2(2), J = 8.1 Hz), 4.22 (t, 2H, N−CH_2, J = 8.1 Hz), 7.82 (s, 1H), 7.92 (s, 1H), 8.03 (d, 1H, H(6′), J = 9.5 Hz), 8.11 (s, 1H), 8.36 (dd, 1H, H(5′), J = 9.5 and 2.6 Hz), 9.17 (d, 1H, H(3′), J = 2.6 Hz), 11.24 (s, 1H, NH). Anal. Calcd for $C_{14}H_{16}N_6O_4$ (mol wt = 332.32): C, 50.6; H, 4.9; N, 25.3. Found: C, 50.7; H, 4.8; N, 25.4.

1-Hexyl-1*H*-pyrazole-4-carbaldehyde was prepared by a procedure similar to that of 1-isopropyl-1*H*-pyrazole-4-carbaldehyde. Yield: 47%. Bp: 116−117 °C (1 Torr). ^{1}H NMR (acetone-d_6): δ 0.87 (distorted t, 3H, CH_3), 1.25−1.45 (m, 6H, $(CH_2)_3$), 1.89 (distorted pentet, 2H, CH_2(2), J = 8 Hz), 4.23 (t, 2H, N−CH_2, J = 8.1 Hz), 7.91 (s, 1H, H(3)), 8.29 (s, 1H, H(5)), 9.85 (s, 1H, CHO). Element analysis was performed for the corresponding dinitrophenylhydrazone as described above. Mp: 165−166 °C. Anal. Calcd for $C_{16}H_{20}N_6O_4$ (mol wt = 360.37): C, 53.3; H, 5.6; N, 23.3. Found: C, 53.3; H, 5.6; N, 23.1.

General Procedure for the Synthesis of 2-(1-Alkyl-1*H*-pyrazol-4-yl)-4,4,5,5-tetramethylimidazolidine-1,3-diols. A mixture of 2,3-bis(hydroxylamino)-2,3-dimethylbutane monosulfate monohydrate (2.50 g, 9.47 mmol) and the corresponding pyrazolecarbaldehyde (7.97 mmol) in water (10 mL) was stirred for 24 h at room temperature and then neutralized with $NaHCO_3$. The product was filtered off and dried in air. **2-(1-Isopropyl-1*H*-pyrazol-4-yl)-4,4,5,5-tetramethylimidazolidine-1,3-diol.** Yield: 2.0 g (94%). Mp: 165−166 °C (AcOEt). IR (cm^{-1}): 741, 794, 817, 845, 889, 917, 949, 960, 991, 1031, 1112, 1144, 1157, 1177, 1188, 1237, 1262, 1326, 1363, 1372, 1385, 1422, 1445, 1465, 1572, 2933, 2979, 3080, 3213. ^{1}H NMR (dmso-d_6): δ 0.99 (s, 6H, C(CH_3)$_2$), 1.02 (s, 6H, C(CH_3)$_2$), 1.37 (d, 6H, CH(CH_3)$_2$, J = 8.2 Hz), the N−CH proton signal coincides with the solvent signal, 4.52 (s, 1H, H(2)), 7.38 (s, 1H, H(3′)), 7.60 (s, 1H, H(5′)), 7.77 (br. s, 2H, 2 HO−N). Anal. Calcd for $C_{13}H_{24}N_4O_2$ (mol wt = 268.36): C, 58.2; H, 9.0; N, 20.9. Found: C, 58.5; H, 9.1; N, 21.0.

2-(1-Butyl-1*H*-pyrazol-4-yl)-4,4,5,5-tetramethylimidazolidine-1,3-diol. Yield: 2.96 g (62%). Mp: 147−148 °C (AcOEt). IR (cm^{-1}): 753, 796, 813, 829, 847, 858, 880, 920, 937, 954, 990, 1007, 1029, 1097, 1120, 1142, 1170, 1245, 1263, 1309, 1340, 1364, 1384, 1436, 1453, 1570, 2872, 2930, 2958, 2986, 3185. ^{1}H NMR ($CDCl_3$): δ 0.93 (t, 3H, CH_3), 0.99 (s, 6H, C(CH_3)$_2$), 1.01 (s, 6H, C(CH_3)$_2$), 1.33 (m, 2H, CH_2), 1.81 (pentet, 2H, CH_2(2), J = 8 Hz), 4.05 (t, 2H, N−CH_2, J = 8 Hz), 4.72 (s, 1H, H(2)), 6.15 (br. s, 2H, 2 HO−N), 7.34 (s, 1H, H(3′)), 7.44 (s, 1H, H(5′)). Anal. Calcd for $C_{14}H_{26}N_4O_2$ (mol wt = 282.39): C, 59.6; H, 9.3; N, 19.8. Found: C, 59.7; H, 9.5; N, 20.0. **2-(1-Hexyl-1*H*-pyrazol-4-yl)-4,4,5,5-tetramethylimidazolidine-1,3-diol.** Yield: 0.44 g (71%). Mp: 136−137 °C (AcOEt). IR (cm^{-1}): 727, 800, 820, 844, 914, 931, 949, 997, 1025, 1107, 1178, 1223, 1242, 1263, 1277, 1318, 1362, 1418, 1462, 1573, 2935, 3080, 3226. ^{1}H NMR ($CDCl_3$): δ 0.86 (t, 3H, CH_3, J = 8 Hz), 0.99 (s, 6H, C(CH_3)$_2$), 1.01 (s, 6H, C(CH_3)$_2$), 1.27−1.48 (m, 6H, $(CH_2)_3$), 1.83 (pentet, 2H, CH_2(2), J = 8 Hz), 4.11 (t, 2H, N−CH_2, J = 8 Hz), 4.72 (s, 1H, H(2)), 6.15 (br. s, 2H, 2 HO−N), 7.34 (s, 1H, H(3′)), 7.44 (s, 1H, H(5′)). Anal. Calcd for $C_{16}H_{30}N_4O_2$ (mol wt = 310.44): C, 61.9; H, 9.7; N, 18.1. Found: C, 62.2; H, 10.1; N, 18.2.

General Procedure for the Synthesis of Pyrazolyl-Substituted Nitronyl Nitroxides. $NaIO_4$ (2.57 g, 0.012 mol) was added in portions for 30 min to a mixture of the appropriate imidazolidine precursor (8.3 mmol), $CHCl_3$ (80 mL), and H_2O (30 mL) stirred at room temperature. After that, the reaction mixture was stirred for another 30 min. The organic layer was separated, and the aqueous layer was extracted with $CHCl_3$ (3 × 15 mL). The combined extracts were dried over Na_2SO_4 and filtered through an Al_2O_3 layer using $CHCl_3$ as an eluent. The solvent was removed in a vacuum. The residue was recrystallized from a 1:5 mixture of benzene and hexane. **2-(1-Isopropyl-1*H*-pyrazol-4-yl)-4,4,5,5-tetramethyl-4,5-dihydro-1*H*-imidazole-3-oxide-1-oxyl (L^1).** Yield: 1.23 g (56%). Mp: 146−147 °C. IR (cm^{-1}): 812, 869, 980, 1016, 1061, 1124, 1173, 1186, 1216, 1310, 1341, 1371, 1404, 1424, 1453, 1484, 1599, 1713, 2970, 3013, 3144. μ_{eff} (β) = 1.73 (295 K). Anal. Calcd for $C_{13}H_{21}N_4O_2$ (mol wt = 265.34): C, 58.9; H, 8.0; N, 21.1. Found: C, 59.1; H, 8.0; N, 21.3. **2-(1-Butyl-1*H*-pyrazol-4-yl)-4,4,5,5-tetramethyl-4,5-dihydro-1*H*-imidazole-3-oxide-1-oxyl (L^2).** Yield: 1.86 g (82%). Mp: 58−59 °C (hexane). IR (cm^{-1}): 650, 665, 756, 812, 868, 978, 1013, 1102, 1126, 1178, 1217, 1306, 1323, 1356, 1405, 1422, 1462, 1484, 1599, 2873, 2953, 3143. μ_{eff} (β) = 1.73 (295 K). Anal. Calcd for $C_{14}H_{23}N_4O_2$ (mol wt = 279.36): C, 60.2; H, 8.3; N, 20.1. Found: C, 60.0; H, 8.5; N, 19.7. **2-(1-Hexyl-1*H*-pyrazol-4-yl)-4,4,5,5-tetramethyl-4,5-dihydro-1*H*-imidazole-3-oxide-1-oxyl (L^3).** For purification, hexane (15 mL) was added to the crude product, and the mixture was heated to boiling and filtered. The filtrate was kept overnight at −15 °C. The cool solvent was decanted. The crystalline product was quickly transferred to a glass filter and dried. Yield: 214 mg (54%). Mp: 47−48 °C (hexane). IR (cm^{-1}): 644, 666, 733, 757, 815, 824, 850, 869, 979, 1017, 1126, 1188, 1217, 1321, 1358, 1400, 1428, 1462, 1487, 1599, 2857, 2930, 3137. μ_{eff} (β) = 1.73 (295 K). Anal. Calcd for $C_{16}H_{27}N_4O_2$ (mol wt = 307.42): C, 62.5; H, 8.9; N, 18.2. Found: C, 62.4; H, 9.0; N, 18.2.

4,4,5,5-Tetramethyl-2-(1-methyl-1*H*-imidazol-5-yl)-4,5-dihydro-1*H*-imidazole-3-oxide-1-oxyl (L^5). A solution of imidazole-4-carbaldehyde (0.96 g, 10 mmol) and dimethyl sulfate (1.26 g, 10 mmol) in EtOH (10 mL) was stirred with boiling for 8 h. The reaction mixture was cooled; water (1 mL) was then added, and the mixture was neutralized with $NaHCO_3$. $CHCl_3$ (20 mL) was then added. The mixture was dried over Na_2SO_4 and filtered through an Al_2O_3 (2 × 10 cm) layer. The solvent was removed. This gave a colorless oil (0.86 g) that was a mixture of 1-methyl-1*H*-imidazole-5-carbaldehyde and 1-methyl-1*H*-imidazole-4-carbaldehyde.[17] MeOH (15 mL) and 2,3-dihydroxyamino-2,3-dimethylbutane (1.48 g, 10 mmol) were added to the mixture of aldehydes. The resulting solution was stirred for 12 h at room temperature; it was then allowed to stay at −10 °C for 24 h. The colorless residue was filtered off and dried in air to give 0.46 g (19% on the basis of imidazole-4-carbaldehyde) of 2-(1-methyl-1*H*-imidazol-5-yl)-

(17) Grimmett, M. R.; Hajos, G.; Karaghiosoff, K.; Mathey, F.; Riedl, Z.; Schmidpeter, A.; Stadbauer, W.; Stanovnik, B.; Svete, J. In *Science of Synthesis: Houben−Weyl Methods of Molecular Transformation, Category 2: Hetarenes and Related Ring Systems*; Neier, R., Ed.; Georg Thieme Verlag: Stuttgart, Germany, 2002; Vol. 12*:* Five-Membered Hetarenes with Two Nitrogen or Phosphorus Atoms, part 12.3.4.3.1.3, p 489.

4,4,5,5-tetramethylimidazolidine-1,3-diol. Mp: 200−204 °C with decomposition. IR (cm^{-1}): 655, 672, 720, 794, 821, 852, 921, 935, 1004, 1031, 1080, 1113, 1139, 1166, 1216, 1239, 1270, 1362, 1377, 1423, 1478, 1518, 2851, 2977, 3012, 3094, 3200. Anal. Calcd for $C_{11}H_{20}N_4O_2$ (mol wt = 240.30): C, 55.0; H, 8.4; N, 23.3. Found: C, 55.2; H, 8.4; N, 23.3. The same product partly stayed in the mother solution along with its isomer, 2-(1-methyl-1*H*-imidazol-4-yl)-4,4,5,5-tetramethylimidazolidine-1,3-diol. This was used for identification of isomers; for this purpose, after the mother solution was evaporated, the residue was oxidized with PbO_2 in MeOH. According to TLC data, the product was a mixture of **L**^{5} and 4,4,5,5-tetramethyl-2-(1-methyl-1*H*-imidazol-4-yl)-4,5-dihydro-1*H*-imidazole-3-oxide-1-oxyl (R_f = 0.4; EtOH, silica gel 60 F_{254} aluminum sheets, Merck), identified by TLC and by comparing with the authentic sample. To prepare the authentic sample, we added NaH (60% in mineral oil, 30 mg, 0.75 mmol) with stirring to a solution of 4,4,5,5-tetramethyl-2-(1*H*-imidazol-4-yl)-4,5-dihydro-1*H*-imidazole-3-oxide-1-oxyl[18] (130 mg, 0.58 mmol) in DMF (2 mL). The reaction mixture was stirred for 15 min. $(CH_3)_2SO_4$ (80 μL) was then added, and the mixture was stirred for another 15 min. The solvent was distilled off at ~1 Torr, and the residue was chromatographed on a SiO_2 (1.5 × 25 cm) column using EtOH as an eluent. Two dark blue fractions were collected. The first fraction contained trace amounts of the starting nitroxide (R_f = 0.5; EtOH, silica gel 60 F_{254} aluminum sheets, Merck). The second was evaporated, and the residue was recrystallized from a benzene−hexane mixture. Crystals suitable for an X-ray analysis were grown from a benzene−heptane mixture. Yield: 80 mg (58%). Dark blue crystals. Mp: 168−169 °C. μ_{eff} (β) = 1.73 (295 K). IR spectrum (cm^{-1}): $\tilde{\nu}$ 631, 648, 665, 691, 756, 827, 868, 922, 1064, 1124, 1146, 1167, 1221, 1236, 1259, 1289, 1333, 1368, 1394, 1413, 1460, 1499, 1587, 1649, 2933, 2983, 3118. Calcd for $C_{11}H_{17}N_4O_2$: C, 55.7; H, 7.2; N, 23.6. Found: C, 56.7; H, 7.3; N, 23.8. Because it was found that condensation of a mixture of aldehydes with 2,3-dihydroxyamino-2,3-dimethylbutane gave 2-(1-methyl-1*H*-imidazol-5-yl)-4,4,5,5-tetramethylimidazolidine-1,3-diol as the only solid substance, this compound (0.46 g, 1.9 mmol) was oxidized with PbO_2 (4.6 g, 19 mmol) in EtOH (46 mL) for 2 h. The reaction mixture was then filtered, and the filtrate was evaporated to yield a fine crystalline product (0.4 g, 88%) containing only **L**^{5} with R_f = 0.8 (EtOH, silica gel 60 F_{254} aluminum sheets, Merck). Mp: 165−166 °C. μ_{eff} (β) = 1.73 (295 K). IR (cm^{-1}): 632, 675, 757, 818, 868, 989, 1051, 1134, 1170, 1211, 1266, 1336, 1367, 1397, 1453, 1516, 1583, 1638, 2992. Anal. Calcd for $C_{11}H_{17}N_4O_2$ (mol wt = 237.28): C, 55.7; H, 7.2; N, 23.6. Found: C, 56.0; H, 6.9; N, 23.8. Blue needles of **L**^{5} of X-ray quality were grown from ethylacetate.

$[Ni_7(OH)_7(C_5H_9O_2)_7(C_5H_{10}O_2)_6(H_2O)]\cdot 0.5C_6H_{14}\cdot 0.5H_2O$ (7), $[Ni_9(OH)_6(C_5H_9O_2)_{12}(C_5H_{10}O_2)_4]\cdot C_5H_{10}O_2\cdot 3H_2O$ (9), $[Ni_6(OH)_4(C_5H_9O_2)_8(C_5H_{10}O_2)_4]$ (6), and $[Ni_8(OH)_4(H_2O)_2(C_5H_9O_2)_{12}]$ (8). An aqueous solution (15 mL) of $C_5H_9O_2K$ (28 g, 0.2 mol) was added at room temperature to a solution of $NiCl_2\cdot 6H_2O$ (27.6 g, 0.12 mol) in water (20 mL). When the solutions were mixed, a light green fine precipitate immediately formed as a suspension throughout the whole volume of the reaction mixture. After being stirred for 1 min, the reaction mixture quickly condensed into dry powder. The powder started to release water in a few seconds. In 2 or 3 min, the resulting wet paste was treated (once) with hexane (60−80 mL). The bright green hexane solution was separated, kept at room temperature for 6−8 h, and filtered. The transparent filtrate was kept for 12−14 h in an open conical flask. After that, the solution diminished to one-half its initial volume. Perfect green crystals **7** were filtered off. From the filtered mass of crystals **7**, single crystals were immediately selected for X-ray investigation and covered with a protective varnish because even after 1 h of storage under normal conditions they started to lose quality and gradually decayed. Yield: 60%. Anal. Calcd for $Ni_7C_{68}H_{140}O_{34.5}$ (mol wt = 1920.7): C, 42.5; H, 7.3. Found: C, 41.8; H, 7.1. Recrystallization of **7** from hexane formed green crystals **9**. Single crystals **9** suitable for an X-ray analysis were selected from under the layer of the mother solution and varnished to protect them from fast decay after storage in air resulting from the loss of solvate molecules. Yield: ~40−50%. Anal. Calcd for $Ni_9C_{85}H_{170}O_{43}$ (mol wt = 2408.5): C, 43.0; H 7.0. Found: C, 42.5; H 7.1. The aqueous phase that remained after the first extraction (during synthesis of **7**) was again treated with hexane (30−40 mL), and the extract was decanted into an open flask. After 2 or 3 days, a film of intergrown fine crystals formed on the walls of the flask, from which it was occasionally possible to separate pale green single crystals. In an X-ray diffraction study, these crystals were identified as $[Ni_6(OH)_4(C_5H_9O_2)_8(C_5H_{10}O_2)_4]$ (**6**) and/or $[Ni_8(OH)_4(H_2O)_2(C_5H_9O_2)_{12}]$ (**8**).

$[Ni_6(OH)_3(C_5H_9O_2)_9(C_5H_{10}O_2)_4(L^4)]\cdot 1.5C_6H_{14}$ (6″). L^4 (0.037 g, 0.216 mmol) mixed with CH_2Cl_2 (5 mL) and hexane (8 mL) was added to a solution of **7** (0.1 g, 0.054 mmol) in CH_2Cl_2 (6 mL). The reaction mixture was stored in an open flask at room temperature for 4 or 5 days. Thin light brown plates formed on the walls of the flask, which could occasionally be separated mechanically for further X-ray studies.

$[Ni_7(OH)_5(C_5H_9O_2)_9(C_5H_{10}O_2)_2(L^1)_2(H_2O)]\cdot 0.5C_6H_{14}\cdot H_2O$ (6+1a), $[Ni_7(OH)_5(C_5H_9O_2)_9(C_5H_{10}O_2)_2(L^2)_2(H_2O)]\cdot H_2O$ (6+1b), $[Ni_7(OH)_5(C_5H_9O_2)_9(C_5H_{10}O_2)_2(L^3)_2(H_2O)]\cdot H_2O$ (6+1c). To a solution of **7** (0.045 mmol) in hexane (10 mL) was added L^1, L^2, or L^3 (0.09 mmol) in hexane (10 mL). The reaction mixture was kept for 3 or 4 days at room temperature. Dark blue crystals of X-ray quality were filtered off, washed with hexane, and dried in air. Yield: 80−90%. (**6**+**1a**): Anal. Calcd for $Ni_7C_{84}H_{159}O_{33}N_8$ (mol wt =2220.0): C, 45.4; H, 7.2; N, 5.0. Found: C, 46.3; H, 7.5; N, 4.9. (**6**+**1b**): Anal. Calcd for $Ni_7C_{83}H_{156}O_{33}N_8$ (mol wt = 2205.0): C, 45.2; H, 7.1; N, 5.0. Found: C, 45.0; H, 7.1; N, 4.9. (**6**+**1c**): Anal. Calcd for $Ni_7C_{87}H_{164}O_{33}N_8$ (mol wt = 2261.1): C, 46.2; H, 7.3; N, 4.9. Found: C, 47.2; H, 7.3; N, 4.8.

$[Ni_4(OH)_3(C_5H_9O_2)_5(C_5H_{10}O_2)_4(L^5)]\cdot 1.5C_7H_8$ (4). To a solution of **7** (0.18 g, 0.096 mmol) in toluene (7 mL) was added L^5 (0.09 g, 0.38 mmol) in toluene (7 mL). The reaction mixture was kept for 5 or 6 days at room temperature; dark blue crystals of X-ray quality were then filtered off. Yield: 50%. Anal. Calcd for desolvated ($Ni_4C_{56}H_{105}O_{23}N_4$) product (mol wt = 1437.2): C, 46.8; H, 7.4; N, 3.9. Found: C, 46.1; H, 7.3; N, 3.8.

Acknowledgment. This work was supported by RFBR (05-03-32095, 05-03-32305, 06-03-08004), CRDF (Y2-C-08-01) grants, RAS, and SB RAS.

Supporting Information Available: Structural determination parameters, crystal and structure refinement data, atomic coordinates, and isotropic displacement parameters for **L**^{1}, **L**^{5}, 4,4,5,5-tetramethyl-2-(1-methyl-1*H*-imidazol-4-yl)-4,5-dihydro-1*H*-imidazole-3-oxide-1-oxyl, **4**, **6**−**9**, **6**″, and **6**+**1a**−**c** (in CIF form). This material is available free of charge via the Internet at http://pubs.acs.org.

IC0522028

(18) Fursova, E. Y.; Ovcharenko, V. I.; Romanenko, G. V.; Tretyakov, E. V. *Tetrahedron Lett.* **2003**, *44*, 6397.